Stem Cell Reports
Article

ISSCR

OPEN ACCESS

Dishevelled 1-Regulated Superpotent Cancer Stem Cells Mediate Wnt Heterogeneity and Tumor Progression in Hepatocellular Carcinoma

Wen-Ying Liao,[1,2,11] Chung-Chi Hsu,[1,3,11] Tze-Sian Chan,[2,4,5,6,11] Chia-Jui Yen,[7] Wei-Yu Chen,[8] Hung-Wei Pan,[3] and Kelvin K. Tsai[1,2,5,6,9,10,*]

[1]Graduate Institute of Clinical Medicine, Taipei Medical University, 250 Wuxing St., Xinyi, Taipei 11031, Taiwan
[2]Laboratory of Advanced Molecular Therapeutics, Taipei Medical University, Taipei 11031, Taiwan
[3]School of Medicine, College of Medicine, I-Shou University, Kaohsiung City 84001, Taiwan
[4]School of Medicine, College of Medicine, Taipei Medical University, Taipei 11031, Taiwan
[5]Division of Gastroenterology, Department of Internal Medicine, Taipei Medical University, Taipei 11031, Taiwan
[6]Integrative Therapy Center for Gastroenterologic Cancers, Taipei Medical University, Taipei 11031, Taiwan
[7]Division of Hemato-oncology, Department of Medicine, National Cheng-Kung University Hospital, Tainan 70403, Taiwan
[8]Department of Pathology, Wan Fang Hospital, Taipei Medical University, Taipei 11031, Taiwan
[9]TMU Research Center of Cancer Translational Medicine, Taipei Medical University, Taipei 11031, Taiwan
[10]National Institute of Cancer Research, National Health Research Institutes (NHRIs), Zhunan 35053, Taiwan
[11]Co-first author
*Correspondence: tsaik@tmu.edu.tw
https://doi.org/10.1016/j.stemcr.2020.02.003

SUMMARY

Various populations of cancer stem cells (CSCs) have been identified in hepatocellular carcinoma (HCC). Wnt signaling is variably activated in HCC and regulates CSCs and tumorigenesis. We explored cell-to-cell Wnt and stemness heterogeneity in HCC by labeling freshly isolated cancer cells with a Wnt-specific reporter, thereby identifying a small subset (0.4%–8.9%) of Wnt-activity^{high} cells. Further cellular subset analysis identified a refined subset of Wnt-activity^{high}ALDH1^{+}EpCAM^{+} triple-positive (TP) cells as the most stem-like, phenotypically plastic, and tumorigenic among all putative CSC populations. These TP "superpotent CSCs" (spCSCs) specifically upregulate the expression of dishevelled 1 (DVL1) through the antagonism between abnormal spindle-like microcephaly-associated (ASPM) and the ubiquitin ligase complex Cullin-3/KLHL-12. Subsequent functional and molecular studies revealed the role of DVL1 in controlling spCSCs and their tumorigenic potential. These findings provide the mechanistic basis of the Wnt and stemness heterogeneity in HCC and highlight the important role of DVL1^{high} spCSCs in tumor progression.

INTRODUCTION

Hepatocellular carcinoma (HCC) is among the most lethal form of solid tumors in humans and affects approximately half a million patients worldwide. Patients with HCC have dismal prognosis owing to the high recurrence rates after surgery or local-regional therapies, as well as the lack of effective therapeutic options for advanced disease (El-Serag and Rudolph, 2007). The multi-kinase inhibitors sorafenib and regorafenib have been approved for the treatment of advanced HCC (Bruix et al., 2017), whereas they only provide a small survival benefit to patients. Recently, the immune checkpoint inhibitor nivolumab has been approved for sorafenib-refractory HCC; however, the overall response rate is low (14.3% on average) (El-Khoueiry et al., 2017). Further advances in the treatment of HCC will rely on a more in-depth understanding of the molecular mechanisms driving HCC aggressiveness, based on which more effective therapeutic strategies can be developed.

Mounting data over recent years have suggested the existence of a subset of cancer cells termed the tumor-initiating cells (TICs) or cancer stem cells (CSCs), which are stem cell-like and have the capability of self-renewing and sustaining tumorigenesis (Batlle and Clevers, 2017). In HCC, various populations of CSCs have been isolated from primary tumors and show distinct characteristics and contribute to tumor growth and metastasis (Tang et al., 2012; Yamashita et al., 2013; Yang et al., 2008). For instance, 30%–40% of HCCs express the epithelial cell adhesion molecule (EpCAM), and the EPCAM^{+} cells display features of hepatic progenitor cells and activated Wnt-β-catenin signaling and are highly tumorigenic (Takai et al., 2019; Yamashita et al., 2008). HCC cells expressing the aldehyde dehydrogenase (ALDH) 1A1 activity or the surface marker CD133 also contain the enriched TIC population (Ma et al., 2007, 2008). On the other hand, HCC cells expressing CD90 display features of vascular endothelial cells and epithelial mesenchymal transition and are highly metastatic (Yamashita et al., 2013). Intriguingly and importantly, a large-scale tumor transcriptomic analysis revealed that HCC-positive for different CSC markers likely represent diverse populations (Gu et al., 2019), highlighting the existence of cell-to-cell heterogeneity in the stemness property of HCC. This paradigm accords with the intratumoral stemness heterogeneity disclosed by large-scale genomic analysis in human malignancies (Malta et al., 2018).

Therefore, the identification of different CSC subsets in HCC along with the elucidation of their functional roles in malignant progression will not only improve our understanding of how cancer stemness is fine-tuned in HCC but also may disclose novel therapeutic targets based on which CSC-targeted therapeutic strategies can be developed and deployed in the clinic.

Wnt signaling has been implicated in epithelial tissue homeostasis by maintaining stem cell proliferation and migration in the intestine, mammary gland, and skin (Clevers and Nusse, 2012). Importantly, the Wnt-regulated self-renewal processes in tissue progenitor and stem cells is frequently hijacked by cancer cells to acquire stem-like phenotype to facilitate malignant progression (Malanchi et al., 2008). Wnt signaling is activated in HCC cells through multiple routes, including function-perturbing mutations in the β-catenin or the *AXIN1* gene (Hoshida et al., 2009; Lachenmayer et al., 2012; Zucman-Rossi et al., 2007) and dysregulated expressions of Wnt receptors, ligands, and/or antagonists (Bengochea et al., 2008). Alternatively, HCC cells can also activate Wnt signaling through the glypican-3-dependent recruitment of Wnt ligands (Gao et al., 2014).

In breast and colorectal cancers, Wnt signaling is not uniformly activated in tumor cells, and there is a considerable degree of heterogeneity in the distribution of cells with high Wnt activity (Cleary et al., 2014; Vermeulen et al., 2010). It is unclear whether human HCC cells also exhibit the cellular heterogeneity in the Wnt activity and, if so, how this heterogeneity is molecularly regulated. To this end, we lentivirally transduced freshly isolated HCC cells with a Wnt-related T cell factor (TCF)/lymphoid enhancer binding factor (LEF) reporter and functionally and molecularly characterized the subset of cells with high β-catenin/TCF/LEF transcriptional activity. Further subset analysis identified a tiny-to-small subset of TCF/LEF transcriptional activity/ALDH1/EPCAM triple-positive (TP) cells as the most tumorigenic, stem cell-like, and phenotypically plastic cells in HCC, which we designated as spCSCs. Molecular screening of Wnt-related factors specifically upregulated in TP spCSCs led to the identification of dishevelled 1 (DVL1) along with its positive regulator abnormal spindle-like microcephaly-associated (ASPM) as their cardinal regulators. The clinical relevance of this finding was underpinned by the significant correlation of the proportion of spCSCs with poor prognosis in patients with HCC. Our findings thus add another level of complexity in the regulation of Wnt activity in HCC, illuminate a tangible and potentially targetable molecular mechanism underlying the Wnt and stemness heterogeneity in HCC, and underscore the importance of interrogating the regional variation in the expression of an oncogenic protein in the progression of HCC.

RESULTS

High Intratumoral Heterogeneity in the Wnt Activity Level in Human HCC

We carried out immunohistochemistry (IHC) analysis on the whole-tumor sections from HCC patients who received surgical removal of their tumors (n = 80; Table S1) and performed single-cell analysis (>100 cells counted per tissue sections; 3 randomly selected sections per tumor) on the expression of the active (non-phosphorylated) form of β-catenin, a well-established marker of activated Wnt signaling. The data revealed that the staining pattern of active β-catenin was highly heterogeneous among individual cancer cells with only an average of 4.1% of them exhibiting a strong (3+) staining intensity (Figure 1A). To gain insights into this tremendous cell-to-cell Wnt heterogeneity, we successfully isolated HCC cells from four patients who received surgical resection of their HCC using a negative selection strategy and lentivirally transduced the purified cells with a Wnt-related TCF/LEF-GFP reporter construct (Figure 1B; Table S2). We ensured that more than 80% of the HCC cells were transduced with the reporter and excluded cells with the background GFP fluorescence signals using a negative control GFP vector during the flow cytometric analysis. As expected, the Wnt-specific reporter activity indeed is highly heterogeneous among primary HCC cells with only a small (0.4%–8.9%) proportion of them exhibiting a bright GFP fluorescence intensity (TCF/LEF-GFP^{bright}; Figures 1C and 1D). Similarly, a small subset (2.6%) of TCF/LEF-GFP^{bright} cells was identified in the established HCC line HuH-1 cells (Figure 1D). Notably, of the four primary cells isolated, only two of them (KVGH-80T and KVGH-90T) could be propagated for an extended period of time (more than ten passages) for the subsequent molecular and functional characterizations (Table S2, bottom). We then sorted TCF/LEF-GFP^{bright} and TCF/LEF-GFP^{dim} KVGH-80T cells by fluorescence-activated cell sorting (FACS) and verified that only the TCF/LEF-GFP^{bright} cells expressed active β-catenin, reflecting activated Wnt signaling in this subset of cells (Figure 1E). Notably, the cell-to-cell heterogeneity in the Wnt activity levels could not be explained by β-catenin mutations as none of the samples or cells examined carry the previously reported function-perturbing β-catenin mutations (Table S3).

Wnt-Activity^{high}ALDH1^{+}EPCAM^{+} HCC Cells Contain the Enriched Population of Highly Tumorigenic and Phenotypically Plastic CSCs

Given the report that CSCs in HCC exhibit a high Wnt signaling activity (Yamashita et al., 2008), we queried if TCF/LEF-GFP^{bright} HCC cells indeed contain the enriched population of CSCs. Consistently, functional studies

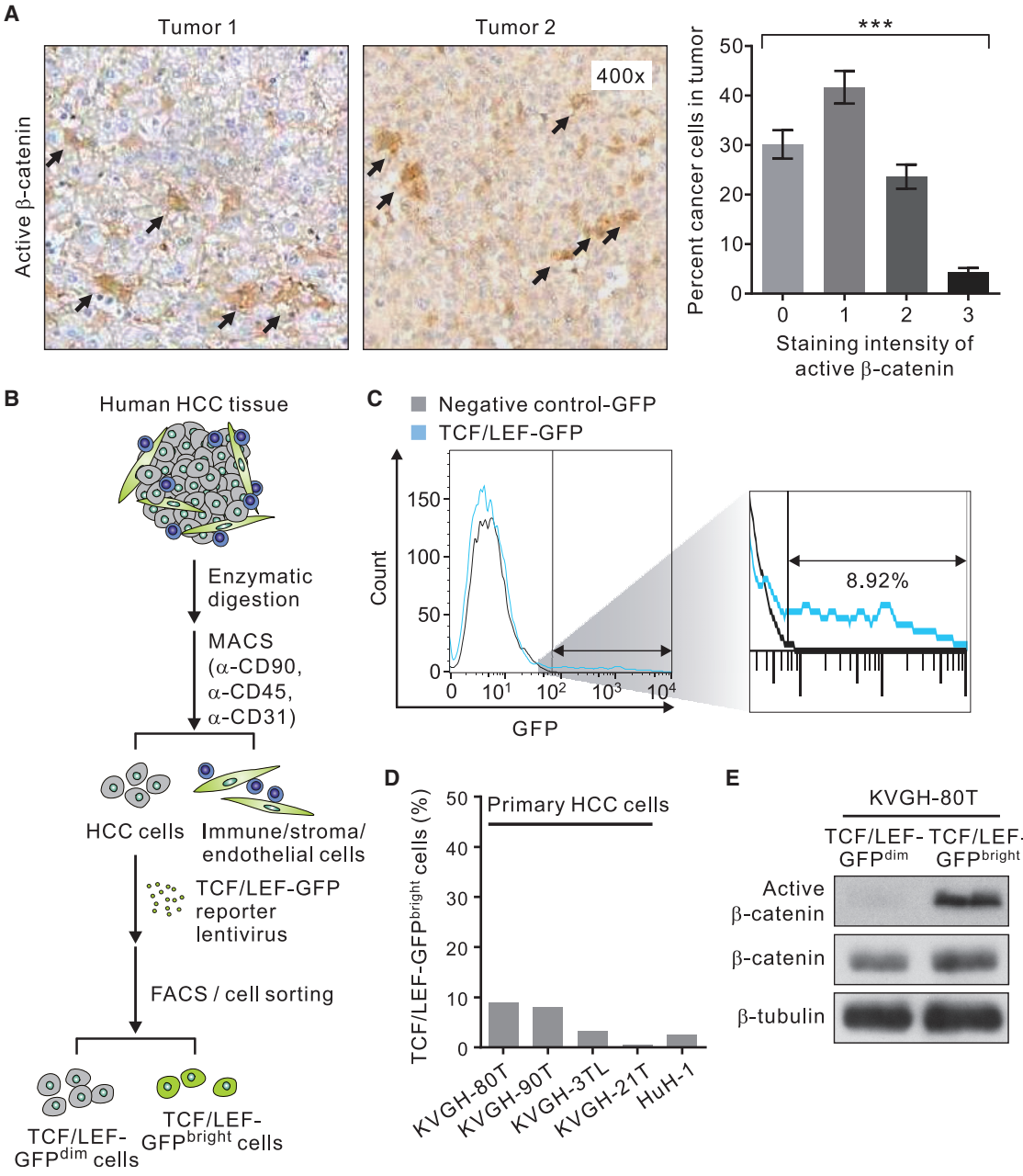

Figure 1. Intratumoral Heterogeneity in Wnt Activity in Human HCC

(A) Representative immunostaining patterns of active β-catenin in human HCC tissues. Right, distribution of the staining intensity of active β-catenin in individual HCC cells in the same tumor. At least 300 tumor cells from 3 different areas were counted per tumor (n = 80 tumors; data are means ± SEM). Arrows, cells exhibiting a strong (3+) staining intensity. ***p < 0.001 by ANOVA.

(B) Schematic illustrating strategy use to isolate primary HCC cells and lentivirally transduce them with the TCF/LEF-GFP reporter (see Experimental Procedures for details).

(C) The identification of TCF/LEF-GFP^{bright} (representing high Wnt activity) HCC cells. Shown is the representative flow cytometry plot illustrating pattern of the GFP signal in freshly isolated KVGH-80T cells lentivirally transduced with TCF/LEF-GFP (light blue line) or a negative control GFP vector (black line).

(D) The percentage of TCF/LEF-GFP^{bright} cells in primary HCC cells, including KVGH-80T, KVGH-90T, KVGH-3TL, and KVGH-21T cells, and the established HCC line HuH-1 cells.

(E) Immunoblotting analysis of active and total β-catenin in TCF/LEF-GFP^{bright} and TCF/LEF-GFP^{dim} KVGH-80T cells. β-Tubulin was included as a loading control.

revealed that TCF/LEF-GFP^{bright} HCC cells had a much higher tumorsphere-forming ability, a functional surrogate for CSC activity, than the GFP^{dim} cells in a quantitative limiting dilution assay (LDA) conducted in the continuously propagatable primary HCC KVGH-80T and KVGH-90T cells (Figure 2A). To verify these *in vitro* findings, we carried out *in vivo* LDA by injecting freshly sorted TCF/LEF-GFP^{bright} or TCF/LEF-GFP^{dim} KVGH-80T cells subcutaneously into the flank of immunodeficient non-obese diabetic/severe combined immunodeficiency (NOD-SCID) mice. Indeed, the TCF/LEF-GFP^{bright} cells have the capability of generating tumors at different dilutions with an average TIC frequency of 1/722 (Figure 2B). By contrast, TCF/LEF-GFP^{dim} cells have a very low TIC frequency (1/34,980).

Interestingly and notably, the freshly labeling of HCC cells with the TCF/LEF-GFP reporter did not identify a distinct subset of HCC cells but a heterogeneous group of GFP^{bright} cells with a widely variation in their GFP fluorescent intensity (see Figure 1C; inset), which, together with the relatively moderate TIC frequency of TCF/LEF-GFP^{bright} HCC cells (1/722; Figure 2B), raised the possibility that a more refined subset of Wnt-active and stem-like TICs may exist in HCC cells. To address this possibility, we simultaneously profiled the TCF/LEF-GFP signal and patterns of expression of ALDH1 and EPCAM, two previously established markers that have been reported to enrich for Wnt-active CSCs in HCC (Cojoc et al., 2015; Yamashita et al., 2008), in primary HCC KVGH-80T cells. We found that the TCF/LEF-GFP reporter, the ALDH1 activity, and the EpCAM marker each identified different but partially overlapping cell populations (Figure 2C), which we verified in the established HCC line HuH-1 cells. Notably, EPCAM^{+} cells comprised a large proportion (57%–82%) of HCC cells; likewise, ALDH1 also marked a considerable proportion (9.4%–33.2%) of the cancer cells. By contrast, the cell subset defined by the TCF/LEF-GFP reporter was relatively small (0.2%–5%). Since de facto CSCs in human malignancies may only comprise a small or even a rare population of cells (Batlle and Clevers, 2017; Pattabiraman and Weinberg, 2014), we sought to identify a more refined subset of HCC cells that have the highest tumorigenic potential by sorting the three subsets of TCF/LEF-GFP^{bright}, ALDH1^{+}, and EPCAM^{+} "single-positive" cells (labeled as population 1 [P1], P2, or P3 in Figure 2C), the three subsets of "double-positive" cells (P5, P6, or P7), the subset of TP cells (P8), and the subset of "triple-negative" cells displaying none of these markers (P4), from primary HCC KVGH-80T and KVGH-90T cells and compared their respective abilities to form tumorspheres (Figure S1A). Among these eight subsets of cells, the TCF/LEF-GFP^{bright}ALDH1^{+}EPCAM^{+} TP cells (i.e., P8) exhibited the strongest ability to form tumorsphere, far exceeding that of the other cellular subsets, in two independently derived primary HCC cells (KVGH-80T and KVGH-90T cells; Figure 2D). At the molecular level, TP cancer cells expressed very high (up to 785-fold compared with non-TP cancer cells) transcript levels of pluripotency- and stemness-related genes (*NOTCH1*, *EZH2*, *KLF4*, *MYC*, *NANOG*, *POU5F1*, and *SOX2*; Figure 2E) and had the strongest ability to form secondary tumorspheres compared with non-TP cells (Figure 2F). Moreover, TP cells were strongly capable of differentiating into most of the other cellular subsets in a time-dependent manner (Figures S1B and 2G), indicating that they are highly phenotypically plastic, which has been linked to the tumorigenic potential of CSCs (Dirkse et al., 2019). Indeed, the TP cells are highly proficient in generating tumors compared with non-TP cells in an *in vivo* LDA performed in NOD-SCID mice (TIC frequency, TP versus non-TP cells: 1/260 versus 1/12,531, $p = 4.03^{-6}$; Figure 2H). These findings collectively suggest that the TCF/LEF-GFP^{bright}ALDH1^{+}EPCAM^{+} TP HCC cells contain the enriched population of spCSCs that may serve as the driving force of HCC tumorigenesis and tumor progression.

Genetic Screening Identified ASPM as a Marker and a Regulator of spCSCs in HCC

To gain further insights into the molecular mechanisms underlying Wnt activation in spCSCs, we compared the transcript levels of 142 unique genes annotated by gene ontology as being related to Wnt signaling pathways (Table S4) between TP spCSCs and non-TP cells sorted from primary HCC KVGH-80T cells using a PCR array or qRT-PCR analysis. This genetic screening identified the gene *ASPM*, which encodes the novel Wnt co-regulator ASPM, as the most upregulated Wnt-associated genes in TP spCSCs in primary HCC cells and HuH-1 cells (Figures 3A and 3B). Previously, a small-scale clinical study has demonstrated the prognostic significance of the transcript level of *ASPM* in human HCC (Lin et al., 2008). However, studies based on analysis on bulk transcript data failed to reveal information regarding the expressional heterogeneity of ASPM, especially that in the small population of CSCs. To profile the cell-to-cell expressional heterogeneity of ASPM, we performed IHC staining of ASPM in multiple randomly selected tissue sections (n = 3 per tumor) from 37 tumors derived from HCC patients who received surgical resection of their tumors in the National Cheng-Kung University Hospital (NCKUH) cohort (Table S1) and carried out meticulous single-cell analyses. Analogous to the expression pattern of active β-catenin (Figure 1A), ASPM expression also displays a considerable cell-to-cell heterogeneity (Figure 3C), with only a small subset (3.7% on average) of the cancer cells displaying a strong (3+) staining intensity. Because spCSCs are found to be both Wnt-activity^{high}

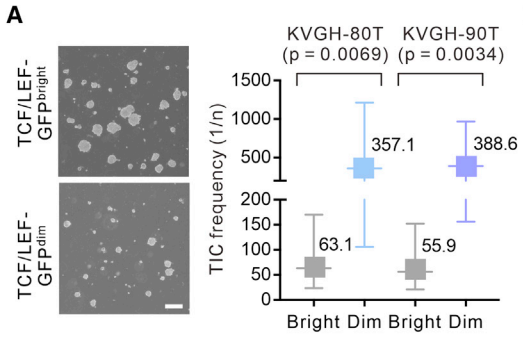

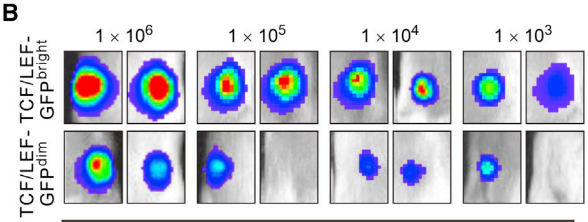

Number of cells	TCF/LEF-GFP^{bright}	TCF/LEF-GFP^{dim}
	Tumor formation	
1 x 10^6	4/4	4/4
1 x 10^5	4/4	2/4
1 x 10^4	4/4	4/4
1 x 10^3	3/4	2/4
TIC frequency^{-1} (95% CI)	722 (213-2454)	34980 (11469-106691)
	p = 1.11^{-6}	

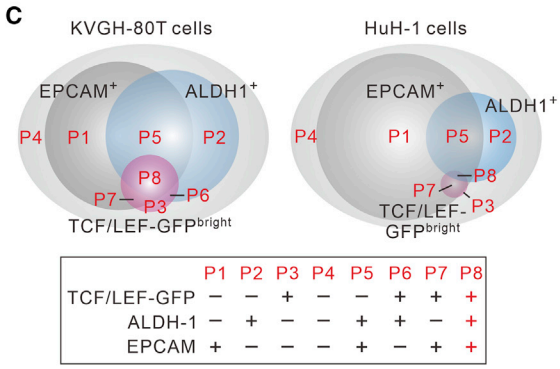

	P1	P2	P3	P4	P5	P6	P7	P8
TCF/LEF-GFP	−	−	+	−	−	+	+	+
ALDH-1	−	+	−	−	+	+	−	+
EPCAM	+	−	−	−	+	−	+	+

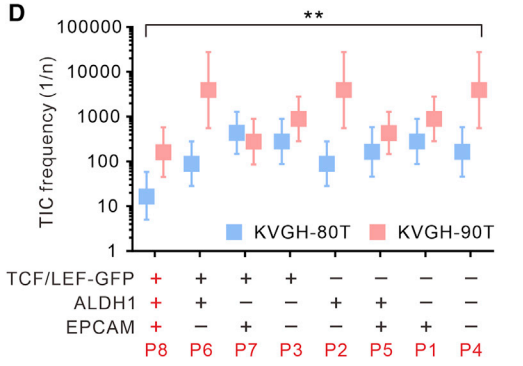

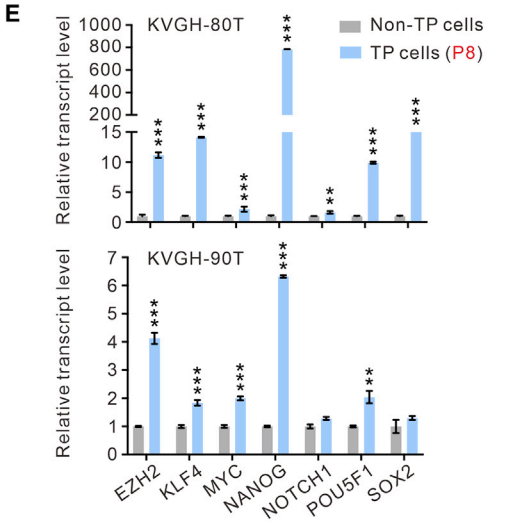

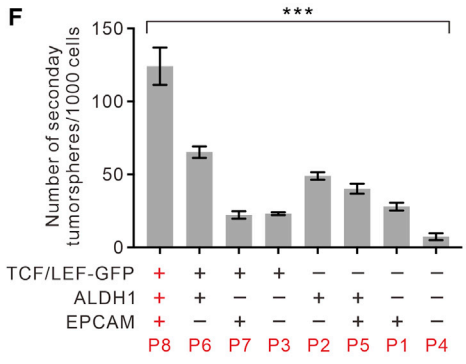

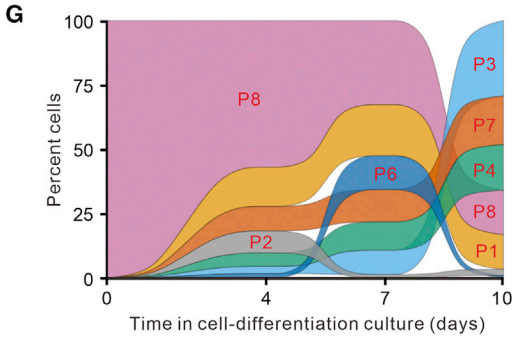

Number of cells	TP cells (P8)	Non-TP cells
	Tumor formation	
1 x 10^6	4/4	4/4
1 x 10^5	4/4	4/4
1 x 10^4	4/4	1/4
1 x 10^3	4/4	2/4
1 x 10^2	1/4	0/4
TIC frequency^{-1} (95% CI)	260 (76.7-887)	12531 (3638.6-43159)
	p = 4.03^{-6}	

(legend on next page)

and ASPM^{high}, we carried out co-immunofluorescence (co-IF) analysis of ASPM and active β-catenin in HCC tissues and confirmed that the HCC cells with high ASPM expression levels strongly colocalized with those with high active β-catenin expression levels (Figure 3D). Indeed, the staining intensity of ASPM among single cancer cells correlated significantly with that of active β-catenin (Spearman correlation = 0.897; $p < 0.001$). Of note, while a large proportion (60%) of cells with a high staining intensity of ASPM also exhibit a moderate-to-bright staining of active β-catenin, a minority (40%) of cells display a low level of active β-catenin expression. These data suggest that ASPM expression partially reflects the Wnt activity in HCC cells, which also may be contributed to by other factors.

Because spCSCs are defined by a fluorescence reporter and two markers (ALDH1 and EPCAM), their detection in human HCC tissues requires gene transduction and are difficult to apply in clinical practice. We thus sought to leverage the ASPM staining as a surrogate marker of spCSCs and explored its potential prognostic utility. We thus denoted the percentage of HCC cells with a moderate-to-strong ASPM staining intensity (≥2+) as the "ASPM staining index (SI)." Indeed, the tumors with a high (>2%; determined using the statistically stringent concordance index [CI]) ASPM SI are associated with a significantly worse survival than those with a lower ASPM SI (log rank $p = 0.0366$; Figure 3E). These data underscore the important role of ASPM/Wnt and stemness heterogeneity in HCC progression and highlight the prognostic importance of spCSCs in HCC.

Our preceding observation that ASPM marks Wnt-activated spCSCs raised the possibility that ASPM may play a role in the regulation of spCSCs. Consistently, knockdown (KD) of *ASPM* expression using lentivirus-mediated transduction of small hairpin RNA (shRNA) (Figure S2A) substantially diminished the population of TP spCSCs and reduced the transcript levels of stemness-associated genes in HCC cells (Figures S2B and S2C). *In vitro* and *in vivo* LDA affirmed that ASPM-deficient HCC cells had a considerably lower tumorsphere-forming capability than the control cells (Figure S2D) and a much lower TIC frequency than that of control-KD cells (Figure S2E). Indeed, KD of *ASPM* expression abrogated the tumorigenic potential of HCC cells implanted subcutaneously into the flank of NOD/SCID mice (Figure S2F).

SpCSCs Upregulate DVL1 Expression through the Antagonism between ASPM and Cullin 3/KLHL12

Our preceding findings of the high expression level of ASPM in TP spCSCs and its role in the maintenance of these Wnt-activity^{high} cells raised the possibility that ASPM may serve as a regulator of Wnt activity in spCSCs. Indeed, KD of *ASPM* expression considerably attenuated Wnt activity (Figure 4A) and markedly reduced the expression levels of a panel of hallmark or liver-specific Wnt/β-catenin target genes (Lachenmayer et al., 2012) in TP spCSCs (Figure 4B). To dissect the mechanism by which ASPM regulates Wnt signaling in spCSCs, we compared the protein abundance levels of a panel of upstream regulators of canonical Wnt signaling (http://web.stanford.edu/group/nusselab/cgi-bin/wnt/) in TP spCSCs freshly sorted from ASPM-KD or control-KD HCC cells. We uncovered that the expressions of β-catenin, DVL1, and casein kinase Iα, was markedly downregulated upon KD of *ASPM* expression (Figure 4C). Intriguingly and notably, the protein abundance levels of other DVL isoforms, including DVL2 or DVL3, were not significantly affected by KD of *ASPM* expression. We verified the findings in both primary HCC cells (KVGH-80T) and established

Figure 2. TCF/LEF-GFP^{bright}ALDH1^{+}EPCAM^{+} Triple-Positive HCC Cells Contain Highly Tumorigenic, Stem-Like, and Phenotypically Plastic CSCs

(A) Freshly sorted TCF/LEF-GFP^{bright} or TCF/LEF-GFP^{dim} primary HCC KVGH-80T or KVGH-90T cells were cultured in serum-free and non-adherent culture plates for 10 days. Shown are representative phase contrast images of the resultant tumorspheres. Scale bar, 200 μm. Right, LDA demonstrating the tumorsphere-forming efficacy (representing TIC frequency *in vitro*; n = 6 biological replicates).

(B) Different doses of TCF/LEF-GFP^{bright} or TCF/LEF-GFP^{dim} KVGH-80T cells were inoculated subcutaneously into the flanks of NOD/SCID mice for the determination of the TIC frequency. Shown on top are representative bioluminescence of the tumors.

(C) Venn diagram illustrating the different cellular subsets defined by the signals of TCF/LEF-GFP, ALDH1, and EPCAM in KVGH-80T or HuH-1 cells.

(D) *In vitro* TIC frequency in the different subsets of primary HCC KVGH-80T or KVGH-90T cells (n = 4 biological replicates).

(E) The transcript levels of the indicated pluripotency- and stemness-associated factors in TCF/LEF-GFP^{bright}ALDH1^{+}EPCAM^{+} triple-positive (TP) KVGH-80T or KVGH-90T cells (i.e., P8 in C) compared with non-TP cells as measured by qRT-PCR (n = 3 biological replicates and n = 3 technical replicas for each condition; data are means ± SEM). $^{**}p < 0.01$; $^{***}p < 0.001$ compared with the bulk cancer cells.

(F) The cells in the tumorspheres formed by the different subsets of KVGH-80T cells were disassociated into single cells and cultivated as secondary tumorspheres. Shown are the frequency of the secondary tumorsphere formation (n = 4 biological replicates; data are means ± SEM). $^{**}p < 0.01$; $^{***}p < 0.001$ by ANOVA in (D) and (F).

(G) Alluvial plot showing the percentage of TP cells (P8) and other subsets of KVGH-80T cells in the cell-differentiation culture over time.

(H) *In vivo* TIC frequency of TP cells and non-TP KVGH-80T cells as determined in (B).

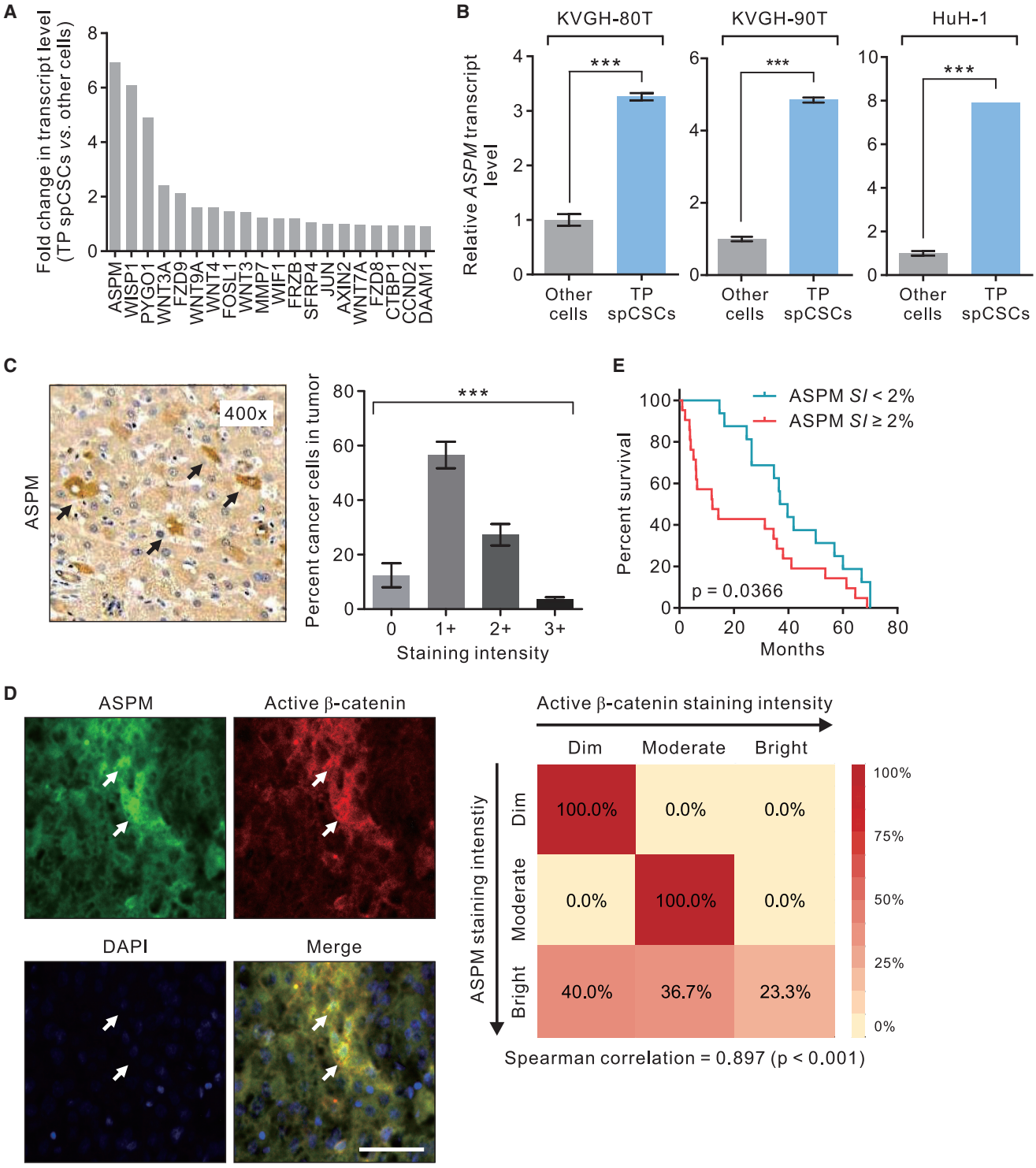

Figure 3. The Identification of ASPM as a Surrogate Marker of spCSCs

(A) Waterfall plot of the top upregulated Wnt-associated genes in TCF/LEF-GFP^{bright}ALDH1^{+}EPCAM^{+} TP spCSCs in primary HCC KVGH-80T cells.

(B) The transcript level of ASPM in TP spCSCs or other cells isolated from KVGH-80T, KVGH-90T, or HuH-1 cells as measured by qRT-PCR analysis (n = 3 biological replicates and n = 3 technical replicas for each condition; data are means ± SEM). ***p < 0.001 compared with other cells.

(legend continued on next page)

cancer lines (HuH-1 and HuH-7 cells; Figure S3). We confirmed the markedly higher protein abundance level of DVL1 in TP spCSCs than in non-TP cells (Figure 4D). DVL1^{high} spCSCs also expressed much higher levels of β-catenin, cyclin D1, and c-Myc, reaffirming the heightened Wnt activity in these cells. Notably, the KD of *ASPM* expression did not affect the transcript level of *CTNNB1* (encoding β-catenin) or *DVL1* (Figure S4), indicating that ASPM specifically regulates their expression at the protein level.

To query if ASPM affects the protein abundance levels of DVL1 and/or β-catenin in a direct or indirect manner, we performed a co-immunoprecipitation (coIP) assay and identified that ASPM physically associated with DVL1 but not with β-catenin, in both primary HCC KVGH-80T and the HCC line HuH-1 cells (Figure 4E). We thus posited that ASPM exerts its Wnt-regulatory function by directly regulating the protein stability of DVL1, which may indirectly lead to the stabilization of the β-catenin protein. Previously, the E3 ubiquitin ligase Cullin 3 has been reported to induce the degradation of DVL2 in glioblastoma cells (Jin et al., 2016). We suspected that Cullin 3 may also be involved in the regulation of DVL1 in HCC cells. Indeed, KD of ASPM expression markedly enhanced the recruitment of Cullin 3 and its adaptor protein Kelch-like 12 (KLHL12) (Angers et al., 2006) to the immunoprecipitated DVL1 protein in TP spCSCs (Figure 4F), leading to a dramatic polyubiquitination of DVL1 (Figure 4G). This in turn led to an enhanced proteasome-dependent degradation of DVL1 as pre-treatment of cells with a proteasome inhibitor could restore its protein abundance level. In line with these biochemical data, co-IF analysis confirmed that the HCC cells with high staining intensities of ASPM significantly colocalized with those with high DVL1 staining (Figure 4H).

DVL1 Is Epistatic to ASPM in Regulating Wnt Activity and spCSCs in HCC Cells

We next sought to elucidate the epistatic relationship between DVL1 and ASPM in the regulation of Wnt activity and spCSCs by stably overexpressing DVL1 in ASPM-deficient HCC cells using lentivirus-mediated gene transduction. The data revealed that, while KD of ASPM reduced the levels of both total and active β-catenin, the stable overexpression (OE) of DVL1 restored their abundance levels in ASPM-deficient HCC cells (Figure 5A). Echoing this molecular study, OE of DVL1 could restore the Wnt-3a-stimulated TCF/LEF luciferase reporter activity in ASPM-deficient HCC cells to approximately 77% of the control-KD cells (Figure 5B). Of note, since our preceding data revealed that ASPM regulates β-catenin indirectly through DVL1 (Figures 4E–4G), the changes in active β-catenin and Wnt activity upon KD of ASPM and/or OE of DVL1 were likely secondary to the changes in the DVL1 protein abundance level. Importantly, OE of DVL1 led to the substantial re-expansion of TP spCSCs in ASPM-deficient HCC cells at a level comparable with or even exceeding control-KD cells (Figure 5C), affirming that DVL1 is epistatic to ASPM in the regulation of spCSCs in HCC cells.

The Mechanistic and Prognostic Roles of DVL1 in spCSCs and HCC Progression

Finally, we sought to corroborate the functional role of DVL1 in spCSCs by stably downregulating its expression using lentivirus-mediated transduction of shRNA (Figure 6A). KD of *DVL1* expression substantially reduced the population of TP spCSCs in wild-type, ASPM-expressing HCC cells (Figure 6B) and considerably inhibited their tumorsphere-forming capacity and TIC frequency (Figure 6C), underscoring the critical role of DVL1 in spCSCs. Next, we carried out IHC analysis on the whole-tumor sections to profile the expression pattern of DVL1 in human HCC tissues. Analogous to the expression patterns of active β-catenin and ASPM, DVL1 expression displayed a considerable cell-to-cell heterogeneity in HCC tissues, with most of the cancer cells displaying a moderate (2+) staining intensity and only a small subset (7% on average) of them displaying a strong (3+) staining intensity (Figure 6D). To evaluate if DVL1^{high} HCC cells are indeed enriched for ASPM^{high} and Wnt-activity^{high} spCSCs, we carried out co-IF analysis of DVL1, ASPM, and active β-catenin in human HCC tissues (Figure 6E). Indeed, the HCC cells with bright DVL1 staining predominantly colocalized with those displaying bright active β-catenin and ASPM staining, with an average of 14.3% (mean ± SEM = 14.3% ± 2.3%) of them being "triple-bright" (i.e., DVL1^{bright}ASPM^{bright}active-β-catenin^{bright}) within the same tumor (see the merged

(C) Representative IHC image showing the heterogeneous expression pattern of ASPM in 37 HCC tissues derived from the patients listed in Table S1. Arrows, cells exhibiting a strong (3+) staining intensity. Right, distribution of the staining intensity of ASPM in the same tumor (data are means ± SEM). ***$p < 0.001$ by ANOVA.

(D) Representative IF images of an HCC tissue immunostained with ASPM (green) and active β-catenin (red). Nuclei were counterstained with DAPI (blue). Arrows, cells simultaneously exhibiting a bright staining of ASPM and active β-catenin (yellow). Scale bar, 50 μm. Right, heatmaps illustrating the correlation of the staining intensity of ASPM and that of active β-catenin in the HCC tissues in (C).

(E) Kaplan-Meier survival curves comparing overall survival of the 37 HCC patients described in (C) stratified according to the percentage of cancer cells with a moderate-to-strong (≥2+) staining intensity of ASPM (ASPM staining index; ASPM SI) within the tumor. The cutoff value of 2% was determined using the concordance index.

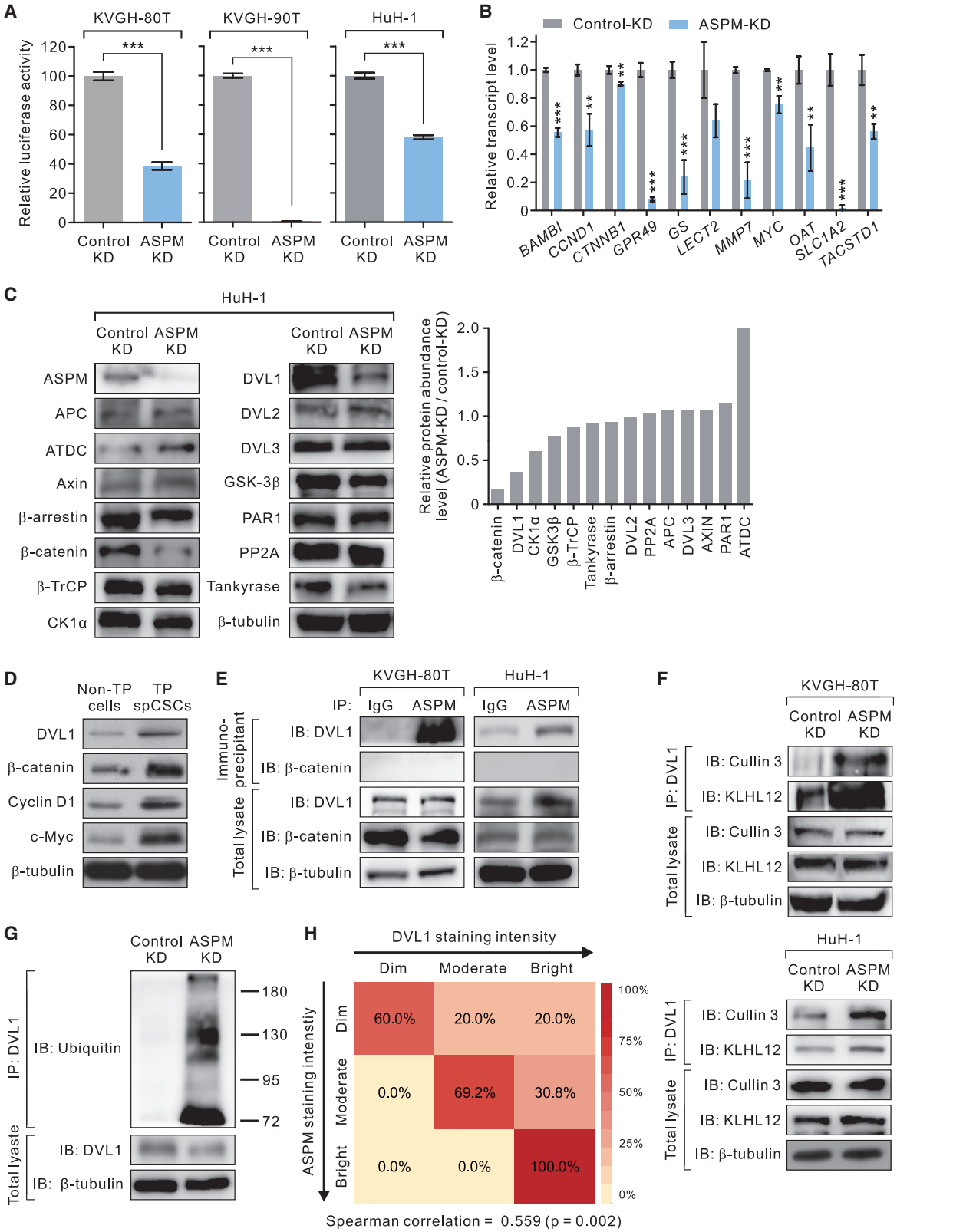

(legend on next page)

IF staining in Figure 6E). The clinical relevance of triple-bright HCC cells, which we reasoned are largely equivalent to TCF/LEF-GFP^{bright}ALDH1^{+}EPCAM^{+} TP spCSCs, was affirmed by the significant inverse correlation of their intratumoral proportion with the overall survival of the 80 HCC patients in the NCKUH cohort (Table S1; Figure 6F). Specifically, the patients with a high percentage of triple-bright cells ($\geq$13.5%), as determined by the statistically robust CI, had a medium survival of 23 months, whereas those with a low percentage (<13.5%) of triple-bright cells had a much longer medium survival of 52 months (log rank p = 0.0001). A multivariable analysis of survival using Cox proportional hazard modeling confirmed that the percentage of triple-bright HCC cells is a significant and independent predictor of survival (hazard ratio [high versus low] = 8.393; 95% confidence interval = 2.852–24.697; p < 0.001), outperforming standard clinico-pathologic variables of HCC (Figure 6G). Taken together, these findings suggest a mechanistic model in which spCSCs in HCC specifically upregulate the expression of ASPM, which competes with Cullin 3/KLHL12 for the binding to DVL1, thereby abrogating its ubiquitination and degradation. The increased DVL1 in spCSCs then procures the Wnt-β-catenin signaling process to positively regulate the stemness and tumorigenic potential of spCSCs, leading to HCC progression (Figure 6H).

DISCUSSION

Malignant tumors typically harbor multiple genetic, phenotypic, and/or functional subclones that compete or cooperate between each other and contribute to the malignant phenotype and influence the therapeutic response of the tumor (Gerlinger et al., 2012; Tabassum and Polyak, 2015). In HCC, various subsets of stem-like and non-stem-like tumor cells co-exist in tumors (Tang et al., 2012; Yamashita et al., 2013; Yang et al., 2008), whereas the molecular mechanisms underlying this phenotypic and functional heterogeneity and the associated pathogenetic significance remain obscure. By labeling freshly isolated HCC cells with a canonical Wnt signaling-specific reporter, we demonstrated the remarkable heterogeneity in Wnt activity in HCC cells and that only a small subset of tumor cells exhibit a strong Wnt activity, which echoed the reported Wnt heterogeneity in other types of cancers (Cleary et al., 2014; Vermeulen et al., 2010). Importantly, by comparing the tumorigenic ability of this newly identified subset of Wnt-activity^{high} cells with that of other previously identified putative CSC subsets in HCC, we identified for the first time a tiny-to-small subset of Wnt-activity^{high}ALDH1^{+}EPCAM^{+} TP spCSCs that have the highest tumorigenic potential and stem-cell-like properties among all HCC cells. Our in-depth molecular and biochemical studies identified DVL1 and its co-regulator ASPM as the major regulators of spCSCs, which provide the first molecularly tractable cell-intrinsic mechanism underlying the Wnt heterogeneity in HCC and emphasize the crucial contribution of Wnt-activated tumor cells to the malignant progression.

The past two decades of investigations into the putative cancer cell populations that fulfill the definition of CSCs in human HCC have identified surrogate markers that enrich potentially different populations of CSCs (Yamashita et al., 2008, 2013). Nevertheless, the pathogenetic significance of these different CSC populations or their mutual relationships have not been rigorously defined. Likewise, substantial variations exist with respect to the prevalence of Wnt activity aberrations as well as the mechanisms giving rise to these aberrations in human HCC (Bengochea et al., 2008; Gao et al., 2014; Hoshida et al., 2009; Lachenmayer et al., 2012;

Figure 4. TCF/LEF-GFP^{bright}ALDH1^{+}EPCAM^{+} TP spCSCs Upregulate DVL1 Expression by the Antagonism between ASPM and the Cullin 3/KLHL12 Complex

(A) Fold Wnt-specific TEC/LEF luciferase expression in control-KD or ASPM-KD and WNT3A (250 ng/mL × 16 h)-treated primary HCC KVGH-80T, KVGH-90T or HuH-1 cells (n = 3 biological replicates and n = 3 technical replicas for each condition; data are means ± SEM). ***p < 0.001.

(B) The transcript levels of the indicated Wnt target genes in control-KD or ASPM-KD and WNT3A-treated KVGH-80T cells (n = 3 biological replicates and n = 3 technical replicas for each condition; data are means ± SEM). **p < 0.01; ***p < 0.001 compared with control-KD.

(C) Immunoblotting analysis of upstream regulators of canonical Wnt signaling in TCF/LEF-GFP^{bright}ALDH1^{+}EPCAM^{+} TP spCSCs in control-KD or ASPM-KD HuH-1 cells. β-Tubulin was included as a loading control. Right, waterfall plot showing the fold of reduction in the protein abundance levels of the proteins analyzed.

(D) IB showing the increased protein abundance levels of DVL1 and the Wnt target genes β-catenin, cyclin D1, and c-Myc in TP spCSCs or non-TP cells sorted from HuH-1 cells. β-Tubulin was included as a loading control.

(E) ASPM interacts with endogenous DVL1 but not with β-catenin in TP spCSCs sorted from HCC KVGH-80T or HuH-1 cells.

(F) KD of *ASPM* expression markedly enhances the recruitment of the E3 ligase Cullin 3 and KLHL12 to the endogenous DVL1 protein in TP spCSCs sorted from KVGH-80T (top) or HuH-1 cells (bottom).

(G) KD of *ASPM* expression resulted in the polyubiquitination of DVL1 in TP spCSCs sorted from HuH-1 cells.

(H) Heatmaps illustrating the correlation of the staining intensity of ASPM and that of DVL1 in HCC tissues (n = 37 tumors). The IF analysis was conducted as in Figure 3D.

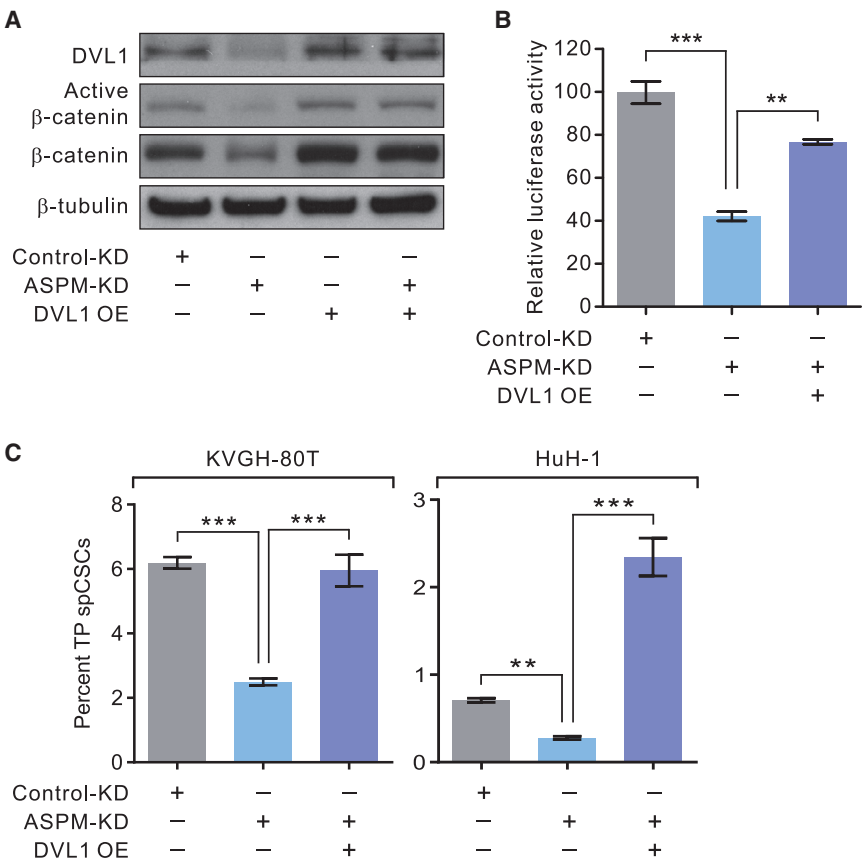

Figure 5. DVL1 Dominantly Regulates Wnt Activity and the Population of spCSCs

(A) Representative IB showing that the stable overexpression (OE) of DVL1 restored the protein abundance level of active and total β-catenin in ASPM-KD HuH-1 cells.

(B) OE of DVL1 restored the Wnt-specific luciferase activity in ASPM-KD HuH-1 cells (n = 3 biological replicates and n = 3 technical replicas for each condition; data are means ± SEM).

(C) OE of DVL1 substantially expanded the population of TP spCSCs in ASPM-KD KVGH-80T or HuH-1 cells (n = 3 biological replicates and n = 3 technical replicas for each condition; data are means ± SEM). **p < 0.01; ***p < 0.001 in (B and C).

Zucman-Rossi et al., 2007). One of the plausible explanations for these highly variable findings is that they were derived from whole-tumor analyses, failing to disclose the intricate cell-to-cell variation that is critical for understanding cancer stemness and Wnt activity as both are associated with tremendous intratumoral heterogeneity (Cleary et al., 2014; Malta et al., 2018). In this regard, this study is the first to investigate the Wnt and stemness heterogeneity in human HCC tissues, and the first to rigorously compare the tumorigenic potential among different HCC cell subsets to identify the most highly tumorigenic, Wnt-active, and stem cell-like CSCs along with their regulatory molecular mechanism. Studies focused on investigating the cellular heterogeneity, like the present one, may illuminate novel tumor compositions and pathogenic pathways that critically control malignant behaviors and the clinical outcome of patients with highly heterogeneous solid tumors such as HCC; said compositions or pathways tend to be overlooked in studies based on whole-tumor analyses.

The DVL proteins are the divergent point and the hub of canonical and non-canonical Wnt signaling (Gao and Chen, 2010). In canonical Wnt signaling, Wnt proteins signal through Frizzled and its coreceptors LRP5/6 to DVL, which in turn inhibits the β-catenin destruction complex of glycogen synthase kinase-3β (GSK3β), axin, and adenomatous polyposis coli (APC), leading to β-catenin-dependent transcription in the nucleus. Because of the importance of DVL in Wnt signaling, studies accumulated over recent years have revealed that DVL is subjected to regulation by multiple cell-intrinsic mechanisms and pathways. For instance, in pancreatic ductal adenocarcinoma (PDAC) cells, ataxia-telangiectasia group D complementing a member of the tripartite motif (TRIM) family, stabilizes DVL2 at the protein level by preventing its proteasome-dependent degradation (Wang et al., 2009). In malignant glioma cells, another TRIM family protein, TRIM14, upregulates the protein level of DVL2, but not DVL1, and thereby activates canonical Wnt signaling and promotes chemoresistance (Tan et al., 2018). In glioblastoma stem cells, the protein stability of DVL2 is indirectly regulated by its E3 ubiquitin ligase, Cullin 3, whose expression is suppressed by the transcriptional repressor inhibitor of differentiation 1 (Jin et al., 2016). These preceding studies were focused on the regulation of DVL2 while ours is the first to identify the specific regulation of DVL1 in CSCs in HCC. Together, these studies unveiled the emerging complexity in the regulation of DVL and Wnt signaling in cancers. How the specificity of the

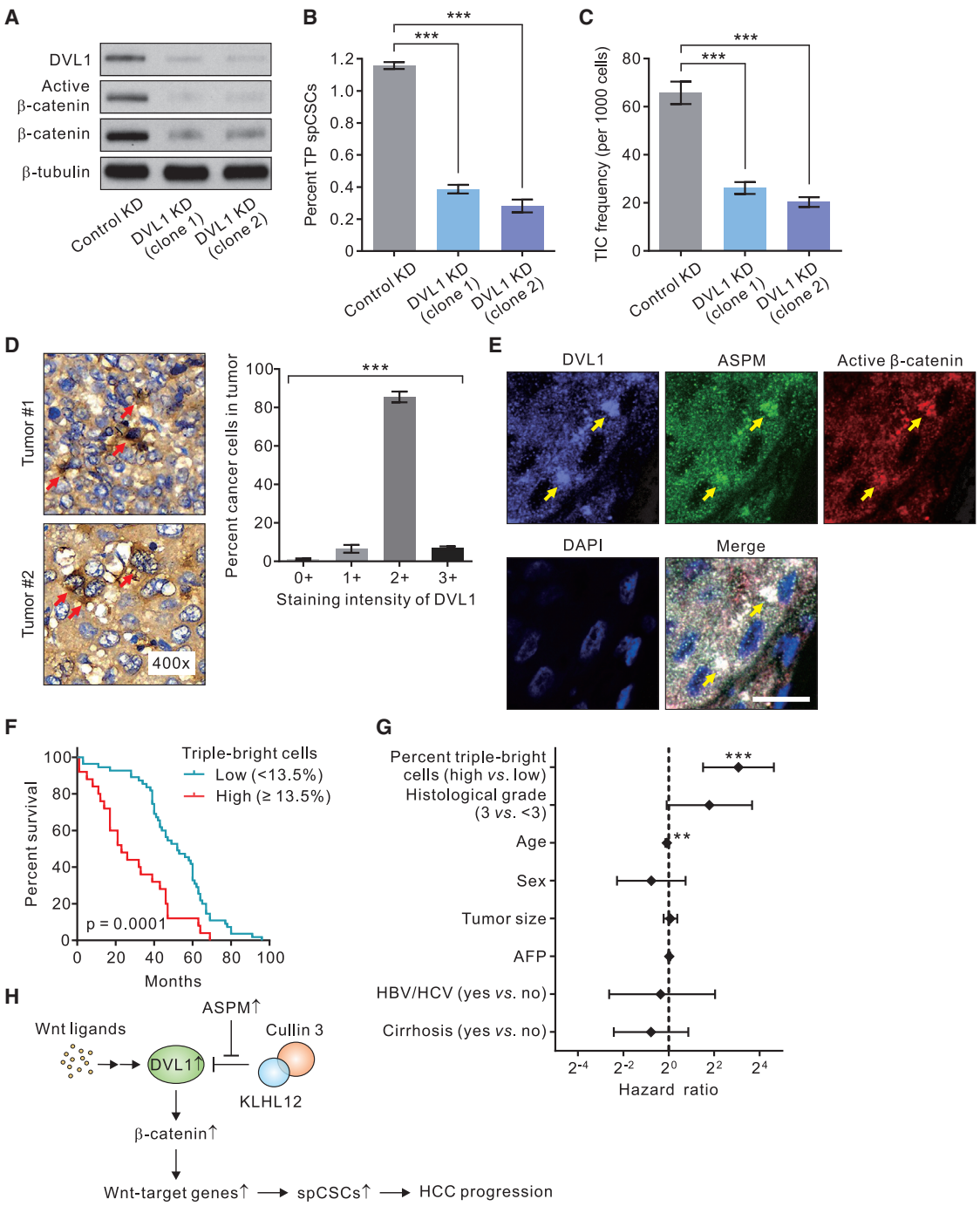

Figure 6. DVL1 Is Indispensable for Wnt-activity^{high} spCSCs and Plays a Prognostic Role in Human HCC

(A) IB showing effect of shRNA-mediated *DVL1* KD in HuH-1 cells. Two different lentivirus shRNA clones were used for the KD.

(B) KD of *DVL1* expression reduced the population of TP spCSCs in HuH-1 cells (n = 3 biological replicates and n = 3 technical replicas for each condition; data are means ± SEM).

(C) KD of *DVL1* expression reduced the tumorsphere-forming efficacy (representing TIC frequency *in vitro*) of HuH-1 cells (n = 4 biological replicates; data are means ± SEM). ***p < 0.001 in (B) and (C).

(D) Representative IHC image showing the heterogeneous expression pattern of DVL1 in human HCC tissues. Arrows, cells with a strong (3+) staining intensity of DVL1. Right, the distribution of the staining intensity of DVL1 in the same tumor. Data are shown as means ± SEM (n = 37 tumors). ***p < 0.001 by ANOVA.

(legend continued on next page)

differential regulatory mechanisms of DVL is conferred in different types of cancer cells, especially CSCs, awaits further in-depth mechanistic investigation.

ASPM was initially identified as a centrosomal protein that regulates neurogenesis and brain size in the central nervous system and is also widely expressed in a variety of normal or malignant tissues (Bruning-Richardson et al., 2011; Kouprina et al., 2005). Several recent studies implicated an oncogenic role of ASPM as its expression correlates with the pathological grade and poor survival in patients with ovarian cancer and PDAC and is overexpressed in approximately 66% of HCC patients (Bruning-Richardson et al., 2011; Hsu et al., 2019; Lin et al., 2008; Wang et al., 2013). Our meticulous immunostaining analysis and Wnt reporter assay conducted on freshly isolated HCC cells are the first to rigorously determine the Wnt activity at the single-cell level, which demonstrated the highly heterogeneous ASPM expression and Wnt activity in human HCC tissues. We further determined that ASPM is highly expressed in spCSCs and that its expression correlates excellently with that of active β-catenin in HCC tissues. These findings suggest that the staining pattern of ASPM can serve as a highly clinical deployable surrogate marker of spCSCs and prognostic markers in HCC. Our subsequent mechanistic studies uncovered that ASPM in spCSCs serves to stabilize the critical Wnt regulator DVL1 through its molecular competition with the E3-ligase complex Cullin 3/KLHL12, thereby inhibiting the degradation of DVL1. Therefore, in ASPM^{high} spCSCs, canonical Wnt ligands are able to initiate the recruitment of DVL1 along with the GSK3β/axin/APC destruction complex to the membrane and thereby stabilize the β-catenin protein, which then directs the expression of Wnt target genes important to pro-stemness and pro-oncogenic functions (Figure 6H). In this model, the epistatic relationship between DVL1 and ASPM was highlighted by our functional rescue experiments in which KD of ASPM expression resulted in a dramatic decrease in the Wnt reporter activity and the abundance of spCSCs, and elevating expression of DVL1 could restore their Wnt activity and re-expand spCSCs in HCC cells.

In summary, our study identifies a novel and tiny-to-small subset of HCC cells that are the most potent in tumorigenesis as a result of ASPM-mediated upregulation of DVL1 expression and augmented Wnt/β-catenin signaling activity. Our results add another level of complexity in the pathogenetic role of aberrant Wnt signaling activity in human HCC and suggest that molecular diagnostics based on the DVL1^{high}Wnt-activity^{high} spCSCs and/or their molecular targeting may provide a new avenue for improving the therapeutic outcome in HCC.

EXPERIMENTAL PROCEDURES

IHC and IF Staining

Formalin-fixed, paraffin-embedded tissues of human HCC from 80 patients who received tumor resection at NCKUH (Tainan, Taiwan; Table S1) were acquired and used in conformity with institutional review board-approved protocols. The processing and the immunostaining of tissue sections is described in the Supplemental Experimental Procedures. IF staining of tissues or cells grown on culture plastics was performed using standard protocols. Confocal imaging was performed using a Nikon Digital Eclipse C1 confocal microscope system. All the IHC and IF stainings were independently evaluated by an experienced researcher (C.-C. Hsu) and an expert pathologist (W.-Y. Chen).

Cell Culture and Staining

Human HCC specimens were excised from four HCC patients who received tumor resection at Kaohsiung Veterans General Hospital (KVGH), Taiwan (Table S2). The isolation of primary HCC cells is described in the Supplemental Experimental Procedures. The freshly isolated HCC cells were cultured in IMDM (Invitrogen) supplemented with glutamine, insulin, transferrin, selenium (all from Lonza), and 20% fetal bovine serum (FBS). Two of the primary cells (KVGH-80T and KVGH-90T cells) could be propagated for more than ten passages to permit subsequent functional and molecular studies. HuH-1 (HBV-related HCC) and HuH-7 (non-B, non-C HCC) cells (Japanese Collection of Research Bioresources; RRID: CVCL-2956) were propagated on tissue culture plastics in DMEM (Invitrogen) supplemented with 10% FBS.

Wnt Signaling Activity Assay

Primary HCC cells or HuH-1 cells were lentivirally transduced with the Cignal Lenti TCF/LEF-GFP reporter, which express GFP under the control of the optimized repeats of the TCF/LEF transcriptional response element, or a negative control GFP reporter (QIAGEN).

(E) Representative IF images of a human HCC tissue immunostained with DVL1 (violet), ASPM (green), and active β-catenin (red). Arrows, cells simultaneously exhibiting a bright staining of DVL1, active β-catenin, and ASPM (triple-bright cells; white). Nuclei were counterstained with DAPI (blue). Scale bar, 50 μm.

(F) Kaplan-Meier survival curves comparing overall survival of 80 HCC patients stratified according to the percentage of DVL1/ASPM/active-β-catenin triple-bright cancer cells (representing spCSCs) within the tumor. The cutoff value of 15% was determined using the Concordance Index.

(G) Forest plots showing hazard ratios (with 95% confidence limits) of death according to the percentage of triple-bright cancer cells or standard clinic-pathological criteria in a Cox proportional-hazards analysis. AFP, alpha-fetoprotein; HBV, hepatitis B; HCV, hepatitis C. $^{**}p < 0.01$; $^{***}p < 0.001$.

(H) Schematic depicting the molecular model by which DVL1 regulates spCSCs and tumor progression in HCC (see Results for details).

GFP$^+$ cells were identified using a FACSCanto™ II flow cytometer (BD Biosciences). A higher than 80% gene transduction rate was verified by infecting the cells with a positive control GFP reporter lentivirus at the same virus titer (QIAGEN).

qRT-PCR and Immunoblotting Analysis

qRT-PCR analysis was performed on the amplified RNA using the LightCycler FastStart DNA MasterPLUS SYBR Green I Kit and the LightCycler System (Roche Diagnostics, Mannheim, Germany) according to the manufacturer's instructions. Primer sequences are shown in Table S5. The transcript levels of 142 unique Wnt-related genes, as identified by gene oncology (Table S4), were determined using the Wnt Signaling Targets PCR Array (QIAGEN, Venlo, Netherlands) or individually using qRT-PCR. Immunoblotting protein analysis was performed according to standard protocols. Antibodies used are listed in Table S6.

Gene Expression Manipulations

Sustained KD of *ASPM* or *DVL1* (encoding DVL1) expression in cells was achieved by lentivirus-mediated RNAi using validated shRNA oligonucleotides in the lentivector pLKO.1-puro (MISSION shRNA lentiviruses; Sigma-Aldrich, St. Louis, MO). The human DVL1 expression vector was purchased from OriGene Technologies (Rockville, MD). The coding sequence of the *DVL1* gene was amplified by PCR and then subcloned into the pLenti-His lentiviral vector (Applied Biological Materials, ABM). Lentivirus was produced in Lenti-X 293T cells (Clontech/Takara Bio, Mountain View, CA, USA) using the packaging vectors pMD2.G (Addgene, no. 12259) and psPAX2 (Addgene, no. 12260) to boost viral titer.

Luciferase Reporter Assay

Cells were lentivirally transduced with Cignal Lenti TCF/LEF luciferase reporter or a negative control luciferase reporter (QIAGEN) according to the manufacturer's protocol. Following stimulation of the cells with recombinant human WNT3A (250 ng/mL for 16 h; R&D Systems, Minneapolis, MN) or vehicle the reporter activity was measured by using the ONE-Glo Luciferase Assay System (Promega, Madison, WI).

Flow Cytometry and Tumorsphere Assays

HCC cells were dissociated, antibody labeled (1–2 μg per 10^6 cells × 1 h), and resuspended in HBSS/2%FBS as described previously (Al-Hajj et al., 2003). Flow cytometry was done used a FACSCanto™ II flow cytometer (BD Biosciences). The ALDEFLUOR assay staining (STEMCELL Techonologies, Vancouver, Canada) or AldeRed 588-A staining (Sigma-Aldrich) was performed according to the manufacturer's recommendation. The tumorsphere assay was performed as described previously (Yamashita et al., 2009). For LDA, FACS-sorted cells were plated in limiting dilution in 96-well plates in the respective culture media. The presence of spheres was evaluated after 15 days.

CoIP Experiments

The antibodies used for coIP experiments are listed in Table S6. coIP was conducted using standard protocols and the proteins were revealed after SDS/PAGE and immunoblotting with indicated antibodies.

Subcutaneous HCC Model

HuH-1 cells were lentivirally transduced using GFP and firefly luciferase (FF-Luc) fusion vector (UBC-EGFP-T2A-Luc; System Biosciences, CA), and the GFP-positive cells were sorted. Cells (1×10^6 cells) were inoculated subcutaneously into the flanks of 8-week-old NOD/SCID mice (BioLASCO Taiwan, Taipei City, Taiwan). The tumor mass and distribution were assessed by bioluminescence (the IVIS Imaging System, Caliper Life Sciences, Waltham, MA).

In Vivo LDA and the Determination of TIC Frequency

In vivo LDA assay was performed as described previously (Yen et al., 2012). Tumor growth was assessed after 28 days. The frequency of tumor growth (take rate) observed at the various cell numbers allow the determination of TIC or CSC frequency using L-Calc version 1.1 software (STEMCELL Technologies). Differences in frequency between groups were analyzed by the likelihood ratio test.

Statistical Analysis

The statistical programming language R (cran.r-project.org) and SPSS 10.0 software (SPSS, Chicago, IL) were used to conduct the statistical analysis of our data. Data for continuous variables are presented as mean ± SEM. A two-tailed Student's t test was used for simple significance testing. A cutoff value that best discriminates between groups with respect to outcome was determined using the CI. Survival curves were generated using the Kaplan-Meier method. The curves were plotted and compared using the log rank test using the GraphPad Prism 5.02 software. The data from the LDA was analyzed and plotted using the ELDA software (http://bioinf.wehi.edu.au/software/elda/index.html). The likelihood ratio test and chi-square test were used to assess the significance.

SUPPLEMENTAL INFORMATION

Supplemental Information can be found online at https://doi.org/10.1016/j.stemcr.2020.02.003.

AUTHOR CONTRIBUTIONS

W.-Y.L, and C.-C.H. performed molecular, biochemistry and cell studies. T.-S.C., W.-Y.C., and H.-W.P. conducted IHC studies and examined the data. W.-Y.L. performed animal works. K.K.T. designed the study, acquired funding, supervised the overall study and wrote the manuscript.

ACKNOWLEDGMENTS

We thank C.-J.Y. for providing us with human HCC tissues. We thank H.-W.P. for providing us with primary HCC cells. This work was supported in part by Ministry of Science and Technology, Taiwan (MOST106-2314-B-038-089-MY3, MOST108-2314-B-038-105-MY3, and MOST108-2314-B-038-026 to K.K.T.; MOST 107-2314-B-038-103 to T.-S.C.), Taipei Medical University (DP2-107-21121-C-04, DP2-107-21121-01-GT-02, 108-TMU-WFH-11, and 108-TMU-WFH-21 to K.K.T.), Wan Fang Hospital, Chi Mei Medical Center, and Hualien Tzu-Chi Hospital Joint Cancer Center Grant,

Ministry of Health and Welfare (MOHW108-TDU-B-212-124020 to K.K.T.), and TMU Research Center of Cancer Translational Medicine from The Featured Areas Research Center Program within the framework of the Higher Education Sprout Project by the Ministry of Education (MOE) in Taiwan (K.K.T.).

Received: August 20, 2019
Revised: February 6, 2020
Accepted: February 10, 2020
Published: March 10, 2020

REFERENCES

Al-Hajj, M., Wicha, M.S., Benito-Hernandez, A., Morrison, S.J., and Clarke, M.F. (2003). Prospective identification of tumorigenic breast cancer cells. Proc. Natl. Acad. Sci. U S A *100*, 3983–3988.

Angers, S., Thorpe, C.J., Biechele, T.L., Goldenberg, S.J., Zheng, N., MacCoss, M.J., and Moon, R.T. (2006). The KLHL12-Cullin-3 ubiquitin ligase negatively regulates the Wnt-beta-catenin pathway by targeting dishevelled for degradation. Nat. Cell Biol. *8*, 348–357.

Batlle, E., and Clevers, H. (2017). Cancer stem cells revisited. Nat. Med. *23*, 1124–1134.

Bengochea, A., de Souza, M.M., Lefrancois, L., Le Roux, E., Galy, O., Chemin, I., Kim, M., Wands, J.R., Trepo, C., Hainaut, P., et al. (2008). Common dysregulation of Wnt/Frizzled receptor elements in human hepatocellular carcinoma. Br. J. Cancer *99*, 143–150.

Bruix, J., Qin, S., Merle, P., Granito, A., Huang, Y.H., Bodoky, G., Pracht, M., Yokosuka, O., Rosmorduc, O., Breder, V., et al. (2017). Regorafenib for patients with hepatocellular carcinoma who progressed on sorafenib treatment (RESORCE): a randomised, double-blind, placebo-controlled, phase 3 trial. Lancet *389*, 56–66.

Bruning-Richardson, A., Bond, J., Alsiary, R., Richardson, J., Cairns, D.A., McCormack, L., Hutson, R., Burns, P., Wilkinson, N., Hall, G.D., et al. (2011). ASPM and microcephalin expression in epithelial ovarian cancer correlates with tumour grade and survival. Br. J. Cancer *104*, 1602–1610.

Cleary, A.S., Leonard, T.L., Gestl, S.A., and Gunther, E.J. (2014). Tumour cell heterogeneity maintained by cooperating subclones in Wnt-driven mammary cancers. Nature *508*, 113–117.

Clevers, H., and Nusse, R. (2012). Wnt/beta-catenin signaling and disease. Cell *149*, 1192–1205.

Cojoc, M., Peitzsch, C., Kurth, I., Trautmann, F., Kunz-Schughart, L.A., Telegeev, G.D., Stakhovsky, E.A., Walker, J.R., Simin, K., Lyle, S., et al. (2015). Aldehyde dehydrogenase is regulated by beta-catenin/TCF and promotes radioresistance in prostate cancer progenitor cells. Cancer Res. *75*, 1482–1494.

Dirkse, A., Golebiewska, A., Buder, T., Nazarov, P.V., Muller, A., Poovathingal, S., Brons, N.H.C., Leite, S., Sauvageot, N., Sarkisjan, D., et al. (2019). Stem cell-associated heterogeneity in glioblastoma results from intrinsic tumor plasticity shaped by the microenvironment. Nat. Commun. *10*, 1787.

El-Khoueiry, A.B., Sangro, B., Yau, T., Crocenzi, T.S., Kudo, M., Hsu, C., Kim, T.Y., Choo, S.P., Trojan, J., Welling, T.H.R., et al. (2017). Nivolumab in patients with advanced hepatocellular carcinoma (CheckMate 040): an open-label, non-comparative, phase 1/2 dose escalation and expansion trial. Lancet *389*, 2492–2502.

El-Serag, H.B., and Rudolph, K.L. (2007). Hepatocellular carcinoma: epidemiology and molecular carcinogenesis. Gastroenterology *132*, 2557–2576.

Gao, C., and Chen, Y.G. (2010). Dishevelled: the hub of Wnt signaling. Cell Signal. *22*, 717–727.

Gao, W., Kim, H., Feng, M., Phung, Y., Xavier, C.P., Rubin, J.S., and Ho, M. (2014). Inactivation of Wnt signaling by a human antibody that recognizes the heparan sulfate chains of glypican-3 for liver cancer therapy. Hepatology *60*, 576–587.

Gerlinger, M., Rowan, A.J., Horswell, S., Math, M., Larkin, J., Endesfelder, D., Gronroos, E., Martinez, P., Matthews, N., Stewart, A., et al. (2012). Intratumor heterogeneity and branched evolution revealed by multiregion sequencing. N. Engl. J. Med. *366*, 883–892.

Gu, Y., Wei, X., Sun, Y., Gao, H., Zheng, X., Wong, L.L., Jin, L., Liu, N., Hernandez, B., Peplowska, K., et al. (2019). miR-192-5p silencing by genetic aberrations is a key event in hepatocellular carcinomas with cancer stem cell features. Cancer Res. *79*, 941–953.

Hoshida, Y., Nijman, S.M., Kobayashi, M., Chan, J.A., Brunet, J.P., Chiang, D.Y., Villanueva, A., Newell, P., Ikeda, K., Hashimoto, M., et al. (2009). Integrative transcriptome analysis reveals common molecular subclasses of human hepatocellular carcinoma. Cancer Res. *69*, 7385–7392.

Hsu, C.C., Liao, W.Y., Chan, T.S., Chen, W.Y., Lee, C.T., Shan, Y.S., Huang, P.J., Hou, Y.C., Li, C.R., and Tsai, K.K. (2019). The differential distributions of ASPM isoforms and their roles in Wnt signaling, cell cycle progression, and pancreatic cancer prognosis. J. Pathol. *249*, 498–508.

Jin, X., Jeon, H.M., Jin, X., Kim, E.J., Yin, J., Jeon, H.Y., Sohn, Y.W., Oh, S.Y., Kim, J.K., Kim, S.H., et al. (2016). The ID1-CULLIN3 axis regulates intracellular SHH and WNT signaling in glioblastoma stem cells. Cell Rep. *16*, 1629–1641.

Kouprina, N., Pavlicek, A., Collins, N.K., Nakano, M., Noskov, V.N., Ohzeki, J., Mochida, G.H., Risinger, J.I., Goldsmith, P., Gunsior, M., et al. (2005). The microcephaly ASPM gene is expressed in proliferating tissues and encodes for a mitotic spindle protein. Hum. Mol. Genet. *14*, 2155–2165.

Lachenmayer, A., Alsinet, C., Savic, R., Cabellos, L., Toffanin, S., Hoshida, Y., Villanueva, A., Minguez, B., Newell, P., Tsai, H.W., et al. (2012). Wnt-pathway activation in two molecular classes of hepatocellular carcinoma and experimental modulation by sorafenib. Clin. Cancer Res. *18*, 4997–5007.

Lin, S.Y., Pan, H.W., Liu, S.H., Jeng, Y.M., Hu, F.C., Peng, S.Y., Lai, P.L., and Hsu, H.C. (2008). ASPM is a novel marker for vascular invasion, early recurrence, and poor prognosis of hepatocellular carcinoma. Clin. Cancer Res. *14*, 4814–4820.

Ma, S., Chan, K.W., Hu, L., Lee, T.K., Wo, J.Y., Ng, I.O., Zheng, B.J., and Guan, X.Y. (2007). Identification and characterization of tumorigenic liver cancer stem/progenitor cells. Gastroenterology *132*, 2542–2556.

Ma, S., Chan, K.W., Lee, T.K., Tang, K.H., Wo, J.Y., Zheng, B.J., and Guan, X.Y. (2008). Aldehyde dehydrogenase discriminates the CD133 liver cancer stem cell populations. Mol. Cancer Res. *6*, 1146–1153.

Malanchi, I., Peinado, H., Kassen, D., Hussenet, T., Metzger, D., Chambon, P., Huber, M., Hohl, D., Cano, A., Birchmeier, W.,

et al. (2008). Cutaneous cancer stem cell maintenance is dependent on beta-catenin signalling. Nature *452*, 650–653.

Malta, T.M., Sokolov, A., Gentles, A.J., Burzykowski, T., Poisson, L., Weinstein, J.N., Kaminska, B., Huelsken, J., Omberg, L., Gevaert, O., et al. (2018). Machine learning identifies stemness features associated with oncogenic dedifferentiation. Cell *173*, 338–354.e15.

Pattabiraman, D.R., and Weinberg, R.A. (2014). Tackling the cancer stem cells—what challenges do they pose? Nat. Rev. Drug Discov. *13*, 497–512.

Tabassum, D.P., and Polyak, K. (2015). Tumorigenesis: it takes a village. Nat. Rev. Cancer *15*, 473–483.

Takai, A., Dang, H., Oishi, N., Khatib, S., Martin, S.P., Dominguez, D.A., Luo, J., Bagni, R., Wu, X., Powell, K., et al. (2019). Genome-wide RNAi screen identifies PMPCB as a therapeutic vulnerability in EpCAM(+) hepatocellular carcinoma. Cancer Res. *79*, 2379–2391.

Tan, Z., Song, L., Wu, W., Zhou, Y., Zhu, J., Wu, G., Cao, L., Song, J., Li, J., and Zhang, W. (2018). TRIM14 promotes chemoresistance in gliomas by activating Wnt/beta-catenin signaling via stabilizing Dvl2. Oncogene *37*, 5403–5415.

Tang, K.H., Ma, S., Lee, T.K., Chan, Y.P., Kwan, P.S., Tong, C.M., Ng, I.O., Man, K., To, K.F., Lai, P.B., et al. (2012). CD133(+) liver tumor-initiating cells promote tumor angiogenesis, growth, and self-renewal through neurotensin/interleukin-8/CXCL1 signaling. Hepatology *55*, 807–820.

Vermeulen, L., De Sousa, E.M.F., van der Heijden, M., Cameron, K., de Jong, J.H., Borovski, T., Tuynman, J.B., Todaro, M., Merz, C., Rodermond, H., et al. (2010). Wnt activity defines colon cancer stem cells and is regulated by the microenvironment. Nat. Cell Biol. *12*, 468–476.

Wang, L., Heidt, D.G., Lee, C.J., Yang, H., Logsdon, C.D., Zhang, L., Fearon, E.R., Ljungman, M., and Simeone, D.M. (2009). Oncogenic function of ATDC in pancreatic cancer through Wnt pathway activation and beta-catenin stabilization. Cancer Cell *15*, 207–219.

Wang, W.Y., Hsu, C.C., Wang, T.Y., Li, C.R., Hou, Y.C., Chu, J.M., Lee, C.T., Liu, M.S., Su, J.J., Jian, K.Y., et al. (2013). A gene expression signature of epithelial tubulogenesis and a role for ASPM in pancreatic tumor progression. Gastroenterology *145*, 1110–1120.

Yamashita, T., Forgues, M., Wang, W., Kim, J.W., Ye, Q., Jia, H., Budhu, A., Zanetti, K.A., Chen, Y., Qin, L.X., et al. (2008). EpCAM and alpha-fetoprotein expression defines novel prognostic subtypes of hepatocellular carcinoma. Cancer Res. *68*, 1451–1461.

Yamashita, T., Honda, M., Nakamoto, Y., Baba, M., Nio, K., Hara, Y., Zeng, S.S., Hayashi, T., Kondo, M., Takatori, H., et al. (2013). Discrete nature of EpCAM+ and CD90+ cancer stem cells in human hepatocellular carcinoma. Hepatology *57*, 1484–1497.

Yamashita, T., Ji, J., Budhu, A., Forgues, M., Yang, W., Wang, H.Y., Jia, H., Ye, Q., Qin, L.X., Wauthier, E., et al. (2009). EpCAM-positive hepatocellular carcinoma cells are tumor-initiating cells with stem/progenitor cell features. Gastroenterology *136*, 1012–1024.

Yang, Z.F., Ho, D.W., Ng, M.N., Lau, C.K., Yu, W.C., Ngai, P., Chu, P.W., Lam, C.T., Poon, R.T., and Fan, S.T. (2008). Significance of CD90+ cancer stem cells in human liver cancer. Cancer Cell *13*, 153–166.

Yen, W.C., Fischer, M.M., Hynes, M., Wu, J., Kim, E., Beviglia, L., Yeung, V.P., Song, X., Kapoun, A.M., Lewicki, J., et al. (2012). Anti-DLL4 has broad spectrum activity in pancreatic cancer dependent on targeting DLL4-Notch signaling in both tumor and vasculature cells. Clin. Cancer Res. *18*, 5374–5386.

Zucman-Rossi, J., Benhamouche, S., Godard, C., Boyault, S., Grimber, G., Balabaud, C., Cunha, A.S., Bioulac-Sage, P., and Perret, C. (2007). Differential effects of inactivated Axin1 and activated beta-catenin mutations in human hepatocellular carcinomas. Oncogene *26*, 774–780.